Cellulose (2018) 25:2381–2391
https://doi.org/10.1007/s10570-018-1719-1

ORIGINAL PAPER

A simple architecture of cellulose microfiber/reduced graphene oxide nanocomposite for the electrochemical determination of nitrobenzene in sewage water

Paramasivam Balasubramanian · T. S. T. Balamurugan · Shen-Ming Chen · Tse-Wei Chen · Tien-Wen Tseng · Bih-Show Lou

Received: 1 October 2017 / Accepted: 21 February 2018 / Published online: 26 February 2018

Abstract Biomaterial nano architectures have become an eminent building block in bio-electronics. A green nano composite of reduced graphene oxide (RGO) supported cellulose microfiber (CMF) was used in an electrochemical assay of nitrobenzene (NB). The synthesized composite was characterized via Fourier Transform Infra-Red spectra, Raman spectroscopy, Scanning electron microscopy and EDX spectroscopy. The CMF-RGO film modified glassy carbon electrode showed promising electrocatalytic activity towards NB reduction in terms of high sensitivity (733.8 μA mM^{-1} cm^{-2}), broad dynamic range (0.2–927.7 μM), and a decent limit of detection (88 nM). On top of this, the composite was used to analyze the water samples collected from river, sewage, and pond aquarium with satisfactory results. In addition, the fabricated sensor matrix offers good durability and appreciable reproducibility. Electrocatalytic performance of the constructed assay was comparable with the reported NB sensors matrices.

Keywords Cellulose microfiber · RGO · Nitrobenzene · Aquatic pollutants · Water analysis

P. Balasubramanian · T. S. T. Balamurugan · S.-M. Chen (✉) · T.-W. Chen · T.-W. Tseng
Department of Chemical Engineering and Biotechnology, National Taipei University of Technology, Taipei 106, Taiwan, ROC
e-mail: smchen78@ms15.hinet.net

T. S. T. Balamurugan
Institute of Biochemical and Biomedical Engineering, National Taipei University of Technology, Taipei 106, Taiwan, ROC

B.-S. Lou (✉)
Chemistry Division, Center for General Education, Chang Gung University, Taoyuan 333, Taiwan, ROC
e-mail: blou@mail.cgu.edu.tw

B.-S. Lou
Department of Nuclear Medicine and Molecular Imaging Center, Chang Gung Memorial Hospital, Taoyuan 333, Taiwan, ROC

Introduction

Nitrobenzene (NB) is an eminent member of aromatic nitro compounds possessing oncogenic activity, a key component of explosives, pesticides, and broadly expelled to environment through dye industries (Zhang et al. 2013). Even a little consumption of NB in eco and biological system is highly hazardous, and causes respiratory diseases, nausea and vomiting (Holder 1999a, b). United States environmental pollution agency (USEPA) categorized NB as a major pollutant and B2 carcinogen fact to their lethal impact over human health and environmental destruction (Wang et al. 2013; Holder and Jinot 1998). These findings uphold the necessity to develop a simple, economic and sensitive tool for the detection of trace level NB from ecological samples. Though, numerous

reformed electrode has been used for the determination of NB over decades (Gupta et al. 2017; Karuppiah et al. 2015; Rastogi et al. 2014; Zhang et al. 2012a, b). However, those projected sensor possess some potential disadvantages such as tedious fabrication procedures and inclusion of high cost noble metals (Au, Pd, Ag, Pt) put a break to their bulk production for day-today commercial application. These above mentioned consequences open up a gate to design and construct a cost effective, reliable NB sensor with high sensitivity and good selectivity.

In recent years, graphene has received great attention in nano technology courtesy to its peculiar optical, electrical, mechanical and structural properties (Allen et al. 2009). The 2D layer structure of sp^2 carbon sheet like structure effectively improving the mechanical and thermal behavior of graphene. Considering their unique properties, graphene has been widely used as a promising and versatile building block for the design of electrode materials for energy storage (Qiu et al. 2016), adsorbent for the removal of organic pollutants (Dong et al. 2018) and electrochemical sensor (Balasubramanian et al. 2017a, b). Moreover, the large delocalized pi-electrons and high specific surface area of the graphene offers a suitable base for embedding carbohydrate polymers (Ouyang et al. 2013). Recently, plentiful effort has been dedicated on and electrically boosted bio polymers with high mechanical strength using graphene sheets as a nano phase (Sadasivuni et al. 2015; Kim et al. 2011; Zhang et al. 2012a, b).

Design and construction of bioelectronics using biomaterials is of great interest in modern era. Cellulose is a highly abundant, biodegradable, biocompatible, and renewable biomaterial derived from plants. It is a long chain polysaccharide of D-glucose polymer linked via β-glycoside linkages. Instead of using petroleum for the synthesis of chemicals and materials, cellulose is thought to be the future feedstock, thanks to its eco-friendly nature and biocompatibility (Habibi 2014). These cellulose polymers based substrates have driven considerable attention in nanotechnology in short time due to their extraordinary physicochemical and mechanical properties (Han et al. 2011). The blend cellulose with conductive materials (graphene, CNT, metal oxides, metal nanoparticles), provides remarkable electrical conductivity, thermal stability, superior stability, of conductive nano mainstay tied with superior biocompatibility of cellulose enable it as a potential candidate in a range of applications such, bio electronics, sensor, adsorption, super capacitor, DSSC, etc., (Weng et al. 2011; Zhang et al. 2015; Qi et al. 2015; Neo and Ouyang 2013). Cellulose incorporated organic–inorganic composites receives significant attention due to their superior physical and chemical properties. For instance, Feng et al. reported a composite of cellulose with graphene improving the mechanical strength and electrical conductivity of the composite material (Feng et al. 2012). Kafy et al., has studied the mechanical and electrical properties of the cellulose grafted graphene (Kafy et al. 2015). Karthik et al. demonstrated that ethyl cellulose greatly enhanced the electro catalytic activity of PtNPs towards the hydrogen peroxide detection (Karthik et al. 2017). Velmurugan et al., developed a NB sensor based on β-cyclodextrin stabilized graphene oxide, and assessed that carbohydrate polymers (β-CD) potentially improved the electro catalytic behaviors of GO towards NB detection (Velmurugan et al. 2017). Velusamy et al., proposed a selective high sensitive hydrogen peroxide sensor via immobilization of hemoglobin on graphene-cellulose microfiber composite, CMF enhanced the solubility and electro catalytic activity of the graphene (Velusamy et al. 2017). Those fascinating observation of the above literatures it is quite obvious that cellulose modified composite materials exhibited superior electro catalytic activity, high ion/electron conductivity with good stability. To our best of knowledge, still now there is no report about cellulose microfiber-reduced graphene oxide as an electro catalyst for the detection of any analyte especially nitrobenzene. Since, the dispersion ability of pristine graphene in aqueous solution is very weak due to its hydrophobic nature. Whereas, the presence of CMF in CMF-RGO composite enhance the dispersion ability of RGO with inclusions of more number of active sites as an additional profit for electrocatalysis.

In this work, we have synthesized reduced graphene oxide supported cellulose microfiber (CMF-RGO) nanocomposite as an electrocatalyst for high sensitive nitrobenzene detection. The polar hydroxyl groups of CMF strongly interact with the defective active sights of reduced graphene oxide, resulting in an enhanced electrocatalytic CMF-RGO composite with high stability. Since, RGO detects the NB at higher oxidation over potential. The CMF-RGO composite modified

glassy carbon electrode showed promising electrocatalytic activity towards NB reduction, which can be attributed by hydrogen bond interaction between CMF and RGO sheets. Moreover, stability, selectivity and practical applicability of the fabricated sensor was studied in detail.

Experimental

Chemicals and instruments

Graphite, cellulose microfiber (CMF), Nitrobenzene ($C_6H_5NO_2$), coffeic acid, disodium hydrogen phosphate (Na_2HPO_4), and sodium dihydrogen phosphate (NaH_2PO_4) were purchased from Sigma Aldrich. All the chemicals and reagents were of analytical rank and used as received. All the electrochemical experiments were carried out in CHI 900 electrochemical work station. Fourier transform infrared (FT-IR) spectra was recorded in JASCO FT/IR-6600 spectrophotometer, and Raman spectral studies carried out in Dong Woo 500i (Korea). The surface morphology of synthesized composite was observed via scanning electron microscopy (SEM) HITACHI S-3000 H. The conventional three electrode system was used for the electrochemical studies, with the modified glassy carbon electrode as a working electrode (electrode surface area: 0.071 cm^2), saturated Ag/AgCl as a reference, and platinum wire as a counter electrode.

Synthesis of CMF-RGO

Graphene oxide was synthesized from graphite following earlier report (Marcano et al. 2010). For the synthesis of CMF-RGO composite, about 10 mL of (1 mg mL^{-1}) homogeneous suspension of graphene oxide was coupled with 50 mg CMF powder and ultrasonicated to obtain a harmonized desperation. About 0.5 mL of coffeic acid (1 M) was added to the mixture of CMF-GO, and continued under sonication for 4 h at 80 °C. The slow and study conversion of stable brown solution into a deep black, indicate the reduction of CMF-GO into CMF-RGO. The black suspension was washed with copious amount of DI water to remove the unreacted traces of precursors and reagent. The resultant CMF-RGO composite was dried at 60 °C for overnight and the obtained CMF-RGO powder was used for further characterizations and electrocatalytic studies.

Preparation of CMF-RGO modified electrode

Prior to electrochemical experiment, glassy carbon electrode was carefully polished with 0.05 mm alumina powder and immersed in HNO_3 to remove oxidizable impurities and washed with water and ethanol. The cleaned electrodes are allowed to dry in air. About, 1 mg of as prepared CMF-RGO composite was dispersed in 1 mL of DI water and sonicated for 10 min to obtain stable CMF-RGO suspension. A pre cleaned mirror like gassy carbon electrode is coated with a freshly prepared suspension of 6 μL CMF-RGO, and dried in air, further referred as CMF-RGO/GCE. RGO/GCE and GCE were taken as control electrodes.

Results and discussion

Structural characterization of CMF-RGO

Scanning electron microscope (SEM) was employed to analyze the dispersion of CMF over graphene matrix and microstructure of CMF-RGO composite. Figure 1A displays SEM delineation of reduced graphene oxide as few layers of ultrafine graphene nanosheets, which are interconnected via Van der Wall's forces with a smooth surface. On the other hand, SEM images of CMF-RGO composite (Fig. 1B) portrayed that surface of reduced graphene oxide turned out rough consist of fine fiber-like structure spread all over the surface. Thus the fibrous surface of composite raised by the hampered coagulation of reduced graphene oxide sheets as CMFs rapidly increase the porous structure of CMF-RGO composite (Neo and Ouyang 2013). The high resolution SEM images of CMF-RGO (Fig. 1C) exhibited homogeneously dispersed wrinkled and crumpled like structure over the surface of the composite, which could facilitate more surface area and could enhance electrocatalytic activity of the CMF-RGO composite. Further, the energy dispersive X-ray spectral (EDX) analysis confirm the elemental composition of CMF-RGO composite. Figure 1D depicts the EDX spectrum of CMF-RGO, it can be seen that corresponding spectrum for carbon and oxygen, with no other

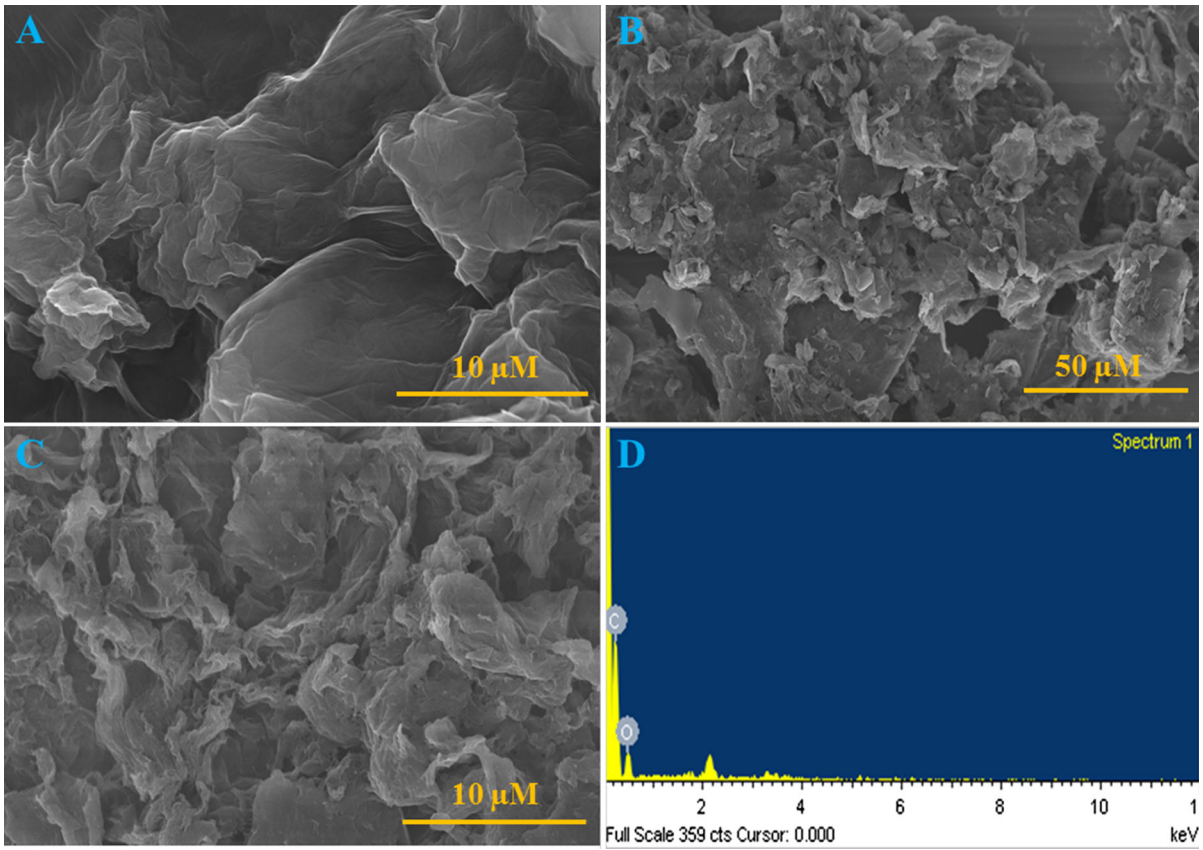

Fig. 1 SEM image of RGO (**A**), CMF-RGO (**B**) and **C** high magnification. **D** The corresponding EDX spectrum of CMR-RGO

elemental impurities from reagents employed for the synthesis. This spectral observations emphasize formation and elemental purity of the composite.

FT-IR spectroscopy has been a significant tool for analyzing the existence and interaction of functional groups present in the nanocomposite. Figure 2A displayed, FT-IR spectroscopy of CMF (red), CMF-RGO (green) RGO (blue). The spectrum of CMF (red) depicts a wide and strong band at 3300–3500 cm^{-1} attributed to the –OH stretching vibration (Zhang et al. 2015). The spectrum also shows peaks at 1049, 1624 and 2914 cm^{-1} assigned to the stretching vibration of C–O–C, C=C, and C–H respectively (Han et al. 2011). The spectrum of reduced graphene oxide (blue) shows

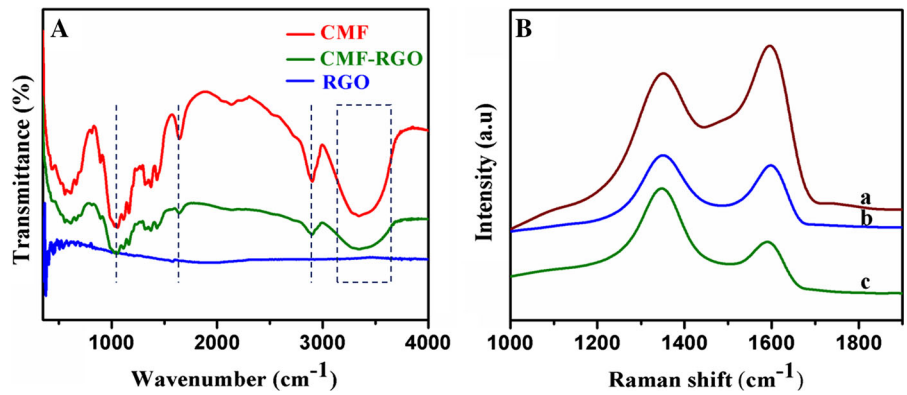

Fig. 2 **A** FT-IR spectra of CMF (red), CMF-RGO (green), and RGO (blue). **B** Raman spectra of GO (a), RGO (b) and CMF-RGO composite (c). (Color figure online)

a characteristic peak at 1598 cm^{-1} indicate there is a C=C bond stretching vibrations in reduced graphene oxide (Vimlesh et al. 2010). In addition, some undistinguished bands in the finger print region are analogous to that of graphene (Palanisamy et al. 2017). On the other hand, typical FT-IR spectrum of CMF-RGO composite (green) also shows characteristic peaks at 1047, 1621 and 2910 cm^{-1}, corresponds to the C–O–C, C=C and C–H stretching respectively, these all characteristic bands indicate that the existence of CMF in CMF-RGO composite (green). These findings confirmed the successful formation of CMF-RGO composite, it has been proved that the series of cellulose microfibers are raised on reduced graphene oxide during the chemical treatment.

Raman spectroscopy is widely exploited to investigate the structural defects in the carbon based materials, especially graphene nanostructures. Raman spectral analysis of GO (a), RGO (b) and CMF-RGO (c) and shown in Fig. 2B. As seen in Fig. 2B. CMF-RGO composite displayed the characteristic D and G bands at around 1349 and 1591 cm^{-1} correspondingly, due to the in-plane vibrational mode of sp^2 hybridized carbon of reduced graphene oxide (Zhao et al. 2012). These findings suggest that the existence of reduced graphene oxide in CMF-RGO composite. The D and G band intensity ratio of GO and RGO to be 0.90 and 1.05 respectively. In contrast, CMF-RGO composite yields a Raman spectrum that has enhanced intensity ratio of D band and G band (1.13), compared with the spectrum of GO and these findings is in agreement with previously reports (Ouyang et al. 2013). The enhanced band intensity ratio of CMF-RGO attributed by the removal of oxygen functional groups of GO during the reduction process resulted in less number of sp^2 carbons in the CMF-RGO composite (Boukhvalov and Katsnelson 2008).

Electrochemical performance of CMF-RGO towards NB reduction

The electrochemical performance of the CMF-RGO composite was evaluated towards NB detection via cyclic voltammetry in 0.05 M PB containing 0.1 mM NB at a scan rate of 50 mV s^{-1}. Figure 3A shows the CV curves of bare GCE (a), RGO/GCE (b), CMF-RGO/GCE (c) towards the NB reduction. The unmodified GCE displayed a faint peak current at − 0.73 V corresponding to the NB reduction and, the RGO/GCE showed a considerable reduction peak with a little enhanced cathodic current at an almost equal peak potential of bare GCE. Interestingly, CMF-RGO/GCE revealed a sharp cathodic peak with enhanced reduction current at a potential of 0.61 V, credits to the direct reduction of nitrobenzene to phenyl hydroxylamine with four electron and proton transfer reaction (Luo et al. 2010). The CMF-RGO/GCE exhibited a six fold higher cathodic current (I_{pc}) associated with minimized over potential of 120 mV lower than formal potential for the reduction of NB in rival with bare GCE, and RGO/GCE. This superior electrocatalytic activity might be attributed by the excellent synergy of CMF and RGO in the composite. In addition, Fig. 3A shows the anodic (II) and cathodic (III) peaks at − 0.04 and − 0.09 V corresponding to the reduction of phenyl hydroxylamine to nitrosobenzene (Velmurugan et al. 2017). These results distinctly exposed that electron transfer ability of the RGO was significantly boosted by successful induction of cellulose polymer into RGO matrix.

Ahead of the electrochemical studies optimizing the amount of CMF loading in CMF-RGO composite towards detection of NB is essential for better electrocatalytic performance. In order to obtain a better electrochemical signal with high sensitivity, various amount of CMF loaded into RGO and obtained current response were shown in Fig. 3B. As shown in Fig. 3B, 5:1 CMF-RGO composite modified electrode delivers maximum current response for the reduction of 0.1 mM NB at a scan rate of 50 mV s^{-1}, then that of control electrodes. Hence, 5 mg mL^{-1} CMF dispersed CMF-RGO composite was used for further electrochemical experiments. The amount of catalyst drop casted on surface of GCE is important; as the amount of catalyst loading could affect the electrocatalytic behavior of the catalyst. The effect of catalyst loading was studied by drop casing various amount of CMF-RGO (3, 4, 5, 6, 7 and 8 μL) on GCE, and dried at room temperature. Figure 3C shows that the current response of 0.1 mM NB in 0.05 M PB solution (pH 7.0) at a scan rate of 50 mV s^{-1}. About, 6 μL of CMF-RGO suspension drop casted GCE showed a maximum current response towards NB reduction than that of other conditions. Hence, 6 μL CMF-RGO drop casted GCE was used for further electrochemical experiments.

The effect of pH over the peak potential and peak current of NB reduction at CMF-RGO modified

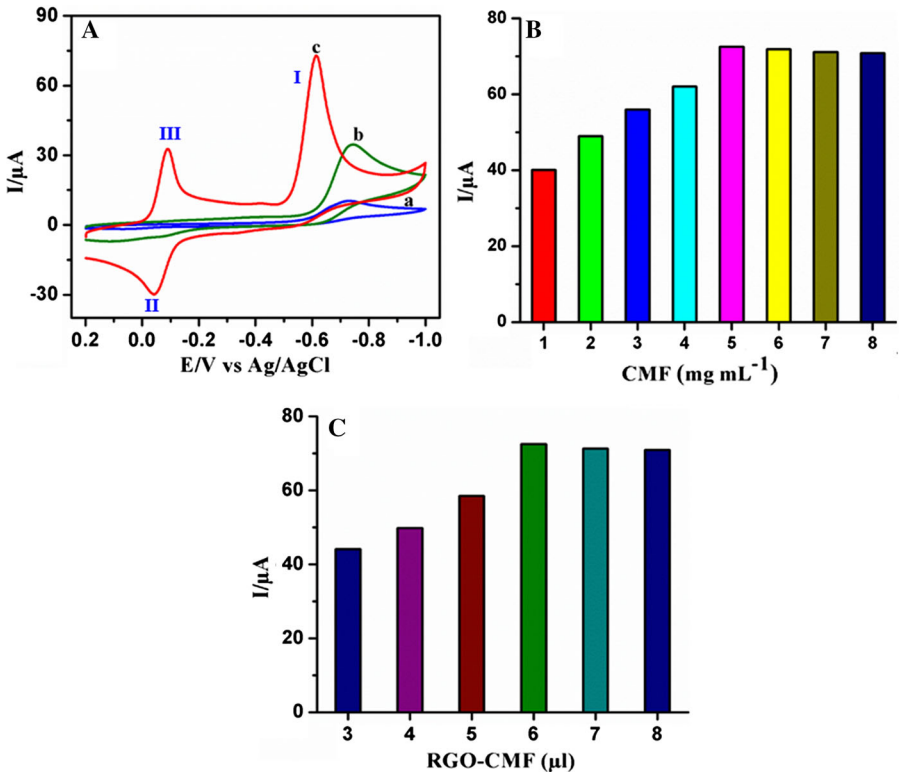

Fig. 3 **A** CV response of the bare GCE (a) and RGO (b), CMF-RGO (c) modified GCE in 0.05 M PB solution containing 0.1 mM NB at a scan rate of 50 mV s^{-1}. **B** The effect of loading of CMF in CMF-RGO composite for the cathodic peak response to 0.1 mM NB. **C** Effect of drop casting of CMF-RGO composite (μL) on GCE for the reduction peak current response to 0.1 mM NB

electrode were studied by CV at various pH (3, 5, 7, 9, 11) in 0.05 M PB solution containing 0.1 mM NB. As seen in the Fig. 4A, increasing the pH from 3 to 7, is in proportion with cathodic current and peak potential of NB reduction. Further hike in pH up to 11, reduction potential shifted to more negative and the cathodic current was decreased (shown in Fig. 4B). These findings suggest that electrochemical behavior of NB depends upon the pH of medium. Figure 4B shows that calibration plot for effect of different pH versus peak potential acquired an excellent correlation coefficient as 0.9948. The maximum cathodic current was obtained at pH 7.0, it may due to the great affection of hydrogen ion concentration to the rate of NB reduction. Hence, pH 7.0 was found to be the optimum pH medium for NB detection.

In order to study the effect of scan rate toward NB reduction by changing the sweep rates. Figure 4C shows, cyclic voltammograms of CMF-RGO/GCE in 0.05 M PB solution containing 0.1 mM NB at various scan rates from 20 to 200 mV s^{-1} (a–j). It is evident that increasing the scan rate, cathodic (I and III) and anodic peak (II) potentials of NB were slightly shifted towards negative and positive pole, respectively. In addition, redox (II and III) and reduction (I) peak currents were increased progressively upon increasing scan rates from 20 to 200 mV s^{-1} (Fig. 4C). These characteristic peaks denoted that NB reduction follows four electron transfer pathway and the oxidation of as-produced secondary product follows two electron transfer pathway at CMF-RGO modified GCE (Ma et al. 2012). Moreover, the cathodic peak current amplification of NB reduction has a linear relationship with square root of the scan rates (Fig. 4D). The obtained linear regression equation expressed as *Ip* (μA) = 7.6034x + 13.695; R^2 = 0.9963. Where *x* is the square root of the scan rate (mV s^{-1})$^{1/2}$. This results indicates that the electrochemical reduction of NB on CMF-RGO modified GCE followed a typical diffusion controlled irreversible electrode process (Rastogi et al. 2014).

Electrochemical determination of NB by DPV

Difference pulse voltammetry (DPV) technique was employed to study the electrochemical assay of NB at CMF-RGO/GCE in 0.05 M PB solution (pH 7.0) at a scan rate of 50 mV s^{-1}. Figure 5A depicted, DPV

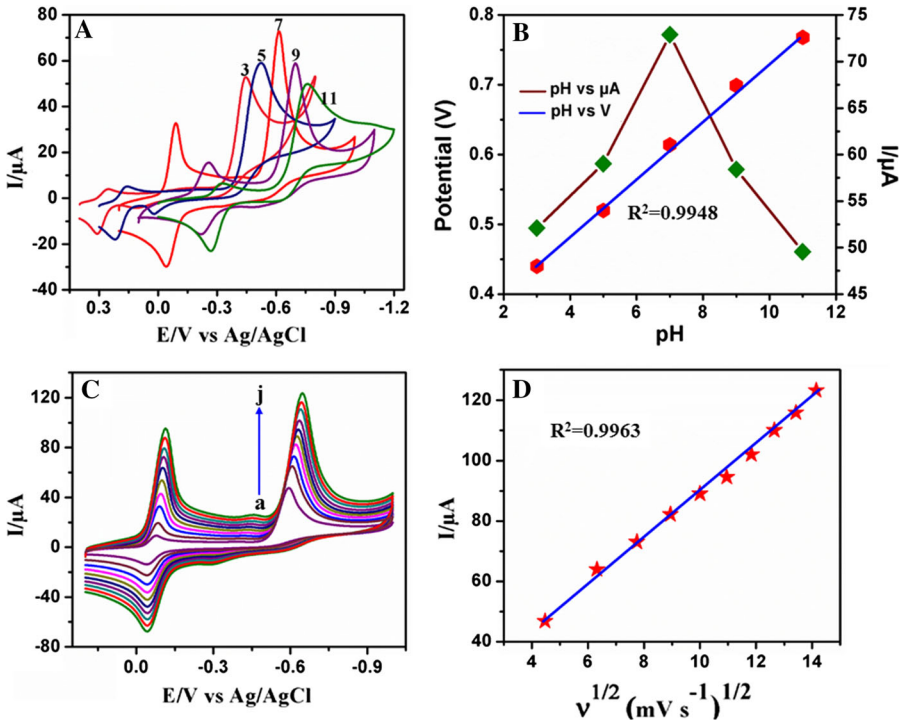

Fig. 4 **A** Cyclic voltammograms of CMF-RGO modified electrode in various pH solutions (0.05 M PB solution) in the presence of 0.1 M NB at a scan rate of 50 mV s^{-1}. **B** The corresponding current responses versus pH of the solution (brown) and obtained cathodic potential versus pH of the buffer (blue). **C** Cyclic voltammograms of CMF-RGO modified electrode in 0.05 M PB solution containing 0.1 mM NB at different scan rates from 20 to 200 mV s^{-1} (a–j). **D** The corresponding linear fit for square root of the scan rate versus cathodic peak current. (Color figure online)

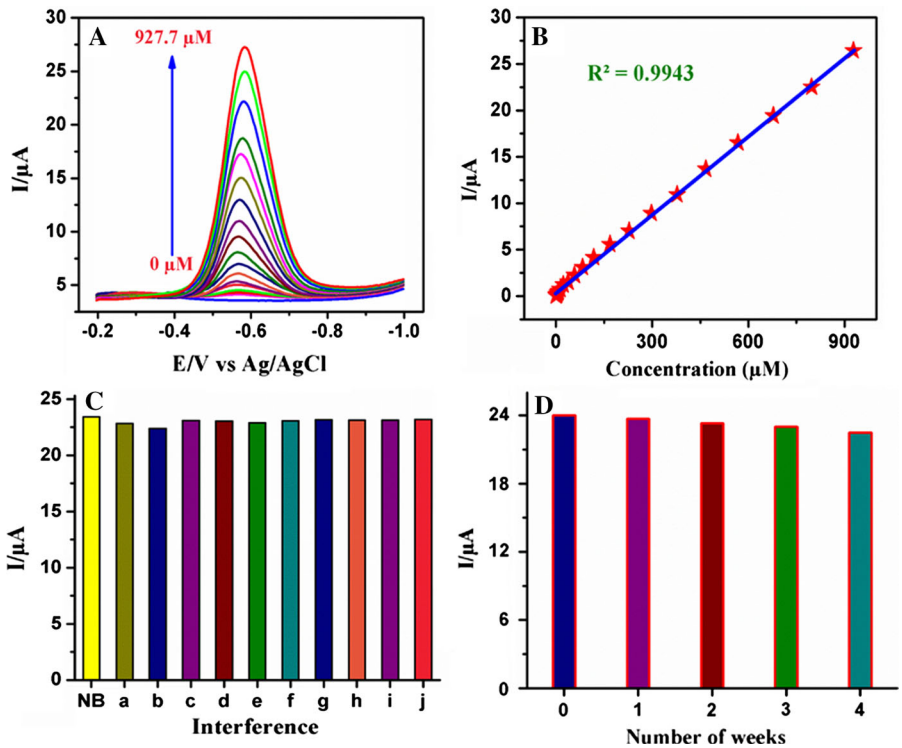

Fig. 5 **A** Typical DPV current response of CMF-RGO modified electrode in absence and presence of various concentration of NB in 0.05 M PB solution (pH 7.0) at a scan rate of 50 mV s^{-1}. **B** The obtained corresponding calibration plot for I_{pa} versus concentration of NB. **C** DPV current response of CMF-RGO modified GCE in the presence of NB with 5 folds concentration of 4-nitrotoluene (a), 4-nitrophenol (b), 4-chloro-nitrobenzene (c), 4-bromo-nitrobenzene (d), 4-nitrobenzoic acid (e) and tenfold concentration of lead (f), cadmium (g), mercury (h), zinc (i), calcium (j). **D** Current response of NB in different time interval

curves of current response of NB reduction at CMF-RGO/GCE. It can be evidently seen that a sharp reduction peak was obtained at a potential − 0.56 V for addition of 0.2 μM NB and linearly increased up to

927.7 μM of NB. The obtained cathodic current response (I_{pc}) were plotted against the concentration of NB (μM) and shown in Fig. 5B. with the linear regression equation of $I_{pc} = 0.0521$ [NB] (μM) + 0.6492. The limit of detection and sensitivity of fabricated electrode was calculated by using the linear plot presented in Fig. 5B. A broad dynamic range of 0.2–927.7 μM was obtained with excellent correlation coefficient of 0.9943. The sensitivity of the sensor was calculated to be 733.8 μA mM^{-1} cm^{-2} and estimated limit of detection to be 88 nM. The observed analytical performance of NB reduction on CMF-RGO/GCE were compared with previously reported NB sensors, shown in Table 1. From these results, as fabricated sensor has excellent electrocatalytic activity toward NB reduction in terms of lower limit of detection, wide dynamic range, and good sensitivity. The excellent electrocatalytic activity of CMF-RGO towards NB reduction, might be attributed to the hydrogen bond interaction between the edges of RGO and polar hydroxyl group of CMF, and the synergy of CMF and RGO in the resultant composite (Weng et al. 2011; Feng et al. 2012; Ouyang et al. 2013).

Selectivity/interference, durability and reproducibility of the sensor

Selectivity is an important parameter of an electrochemical sensor as the poisoning species significantly affects the sensitivity and lower limit of detection of the electrode; poisoning species will intermingle with analyte and electrode materials to form unwanted products thus, resulted in poor sensitivity and selectivity. The selectivity of the designed sensor was studied in presence of various nitro aromatic compounds, and some potentially interfering metal ions. DPV was performed in 0.05 M PB solution (pH 7.0) solution containing NB with fivefolds of nitro aromatic compounds such as 4-nitrotoluene (a), 4-nitrophenol (b), 4-chloro-nitrobenzene (c), 4-bromo-nitrobenzene (d), 4-nitrobenzoic acid (e) and tenfolds of metal ions such as lead (f), cadmium (g), mercury (h), zinc (i), calcium (j) in the presence of NB. The obtained reduction current response of NB in presence of above mentioned interference species were shown in Fig. 5C. It can be seen that, there is a slight change (3–5%) on cathodic peak current of NB reduction in the presence of poisoning species. Commonly, graphene based materials potentially interact with various interfering species and compounds, herein the introduction of CMF led to selective interaction with

Table 1 Comparison of analytical parameters of CMF-RGO modified GCE with earlier reported sensors for NB determination

Electrode material	Linear range (μM)	LOD (μM)	References
β-CD/GO/SPCE	0.5–100	0.184	Velmurugan et al. (2017)
RGO–AgNPs/GCE	0.5–900	0.26	Karuppiah et al. (2015)
TPDT-Ag NPs	–	5	Rameshkumar et al. (2014)
Pd-GG-g-PAM-silica/GCE	1.0–1900	0.06	Rastogi et al. (2014)
Au-MOF-5/GCE	20–500	15.3	Yadav et al. (2016)
OMCN-800/GCE	4–40	1.52	Zhang et al. (2014)
Ag/ATP/GCE	3–30	1.1	Liang et al. (2011)
OMC/DDAB/GCE	25–2900	10	Qi et al. (2008)
PAA–AgNPs/GCE	10–600	1.68	Kariuki et al. (2016)
BiF/CPE	1–100	0.830	Luo et al. (2010)
GCE/Au-MOF-5	20–500	15.3	Yadav et al. (2016)
GCE/TPDT-Ag NPs	–	0.1	Rameshkumar et al. (2014)
CMF-RGO	0.2–927.7	0.088	This work

β-CD β-cyclodextrin, *RGO* reduced graphene oxide, *AgNPs* silver nanoparticles, *OMCN* ordered mesoporous carbon nitride, *Ag/ATP* attapulgite-silver, *PAA* poly(amic) acid, *BiF/CPE* bismuth-film modified carbon paste electrode, *Au-MOF-5* gold nanoparticles-metal organic framework, *TPDT* N-[3-(trimethoxysilyl)propyl] diethylenetriamine

NB. This results shows that CMF-RGO modified electrode possess excellent selectivity toward NB detection.

The stability of a newly fabricated sensor is an important factor for further application. The storage stability of the sensor was studied carried out about 1 month and the sensor retains about 97% of the initial current response of NB reduction after 30 days (Fig. 5D). Moreover, the operational stability of the proposed sensor was evaluated by 100 concordant cycles were obtained in the presence of 0.1 mM of NB in 0.05 M PB solution at a scan rate of 50 mV s^{-1} and shown in Fig. 6. Herein, the attained current of first cycle for NB reduction almost retained, about 5.4% of reduction current only drops. These results suggest that CMF-RGO/GCE has appreciable operational stability as well as excellent storage stability. To study the reproducibility of the sensor by three various CMF-RGO/GCE were prepared under similar condition. The fabricated all electrodes shows almost same cathodic current response of NB reduction with a relative standard deviation of 2.92% (RSD). This results reveals that the CMF-RGO/GCE holds excellent reproducibility.

Detection of NB in real water samples

The practical applicability of the CMF-RGO based sensor was evaluated using river and city sewage water samples, collected from Xindian River (Taipei, Taiwan), Taipei city sewage, and Taipei Tech pond aquarium respectively. Before the experiment, water samples are just centrifuged to remove any suspended impurities. DPV method was performed for real time detection of NB, there is no NB traces were found in river, city sewage, and pond aquarium samples. Further, the recovery rate was observed by spiked samples with using standard addition method. The observed recovery results to be about 96.1–100.9%, results were summarized in Table 2. As shown in Table 2, proposed CMF-RGO based NB sensor offered acceptable recovery results and it could be used for direct environmental analysis.

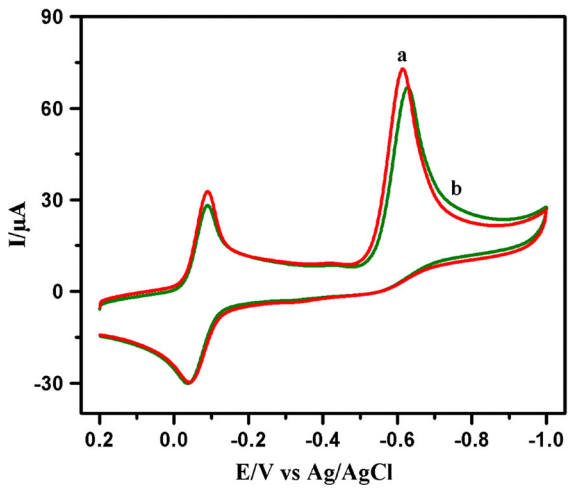

Fig. 6 Cyclic voltammograms of CMF-RGO modified electrode in first (a) and 100th cycle (b)

Table 2 Real time detection of NB in river water and sewage water samples at CMF-RGO modified electrode

Sample	Added (μM)	Found (μM) (n = 3)	RR (%)
River water	–	–	–
	0.5	0.496	99.2
	1	9.98	99.8
Sewage water	–	–	–
	0.5	0.48	96.1
	1	0.979	97.9
Pond water	–	–	–
	0.25	0.246	98.4
	0.75	0.743	100.9

Conclusion

An affordable NB sensor has been fabricated via green synthesized CMF-RGO composite. Formation of CMF-RGO composite was confirmed via systematic physicochemical characterizations. The architected sensor exhibited excellent electrocatalytic activity toward NB reduction. The fabricated sensor showed a minimized reduction potential (− 0.61 V), nanomolar detection (88 nM), with broad linear range (0.2–927.7 μM) towards NB detection. The results were superior to previously reported NB sensors. Moreover, the fabricated sensor offers good durability and reproducibility. The practicality of the sensor was demonstrated in various water samples with satisfactory results.

Acknowledgments The authors gratefully acknowledge the financial support of the Ministry of Science and Technology, Taiwan through Contract Nos: MOST106-2113-M-027-003 and

MOST106-2221-E-182-021. The financial support from the Chung Gung Memorial Hospital through Contract No. BMRP 280 to B.S. Lou is also acknowledged.

References

Allen MJ, Tung VC, Kaner RB (2009) Honeycomb carbon: a review of graphene. Chem Rev 110:132–145

Balasubramanian P, Velmurugan M, Chen SM et al (2017a) Optimized electrochemical synthesis of copper nanoparticles decorated reduced graphene oxide: application for enzymeless determination of glucose in human blood. J Electroanal Chem 807:128–136

Balasubramanian P, Thirumalraj B, Chen SM et al (2017b) Electrochemical determination of isoniazid using gallic acid supported reduced graphene oxide. J Electrochem Soc 164:H503–H508

Boukhvalov DW, Katsnelson MI (2008) Modeling of graphite oxide. J Am Chem Soc 130:10697–10701

Dong C, Lu J, Qiu B et al (2018) Developing stretchable and graphene-oxide-based hydrogel for the removal of organic pollutants and metal ions. Appl Catal B Environ 222:146–156

Feng Y, Zhang X, Shen Y et al (2012) A mechanically strong, flexible and conductive film based on bacterial cellulose/graphene nanocomposite. Carbohydr Polym 87:644–649

Gupta R, Rastogi PK, Ganesan V et al (2017) Gold nanoparticles decorated mesoporous silica microspheres: a proficient electrochemical sensing scaffold for hydrazine and nitrobenzene. Sens Actuat B 239:970–978

Habibi Y (2014) Key advances in the chemical modification of nanocelluloses. Chem Soc Rev 43:1519–1542

Han D, Yan L, Chen W et al (2011) Cellulose/graphite oxide composite films with improved mechanical properties over a wide range of temperature. Carbohydr Polym 83:966–972

Holder JW (1999a) Nitrobenzene potential human cancer risk based on animal studies. Toxicol Ind Health 15:5

Holder JW (1999b) Nitrobenzene carcinogenicity in animals and human hazard evaluation. Toxicol Ind Health 15:5

Holder J, Jinot J (1998) National center for environmental assessment, Washington. Office, Washington, EPA/600/R-95/100

Kafy A, Sadasivuni KK, Akther A et al (2015) Cellulose/graphene nanocomposite as multifunctional electronic and solvent sensor material. Mater Lett 159:20–23

Kariuki VM, Fasih-Ahmad SA, Osonga FJ et al (2016) An electrochemical sensor for nitrobenzene using π-conjugated polymer-embedded nanosilver. Analyst 141:2259–2269

Karthik R, Karikalan N, Chen SM (2017) Rapid synthesis of ethyl cellulose supported platinum nanoparticles for the non-enzymatic determination of H_2O_2. Carbohydr Polym 164:102–108

Karuppiah C, Muthupandi K, Chen SM et al (2015) Green synthesized silver nanoparticles decorated on reduced graphene oxide for enhanced electrochemical sensing of nitrobenzene in waste water samples. RSC Adv 5:31139–31146

Kim CJ, Khan W, Kim DH et al (2011) Graphene oxide/cellulose composite using NMMO monohydrate. Carbohydr Polym 86:903–909

Liang F, Liu B, Deng Y et al (2011) Preparation and characterization of attapulgite-silver nanocomposites, and their application to the electrochemical determination of nitrobenzene. Microchim Acta 174:407

Luo L, Wang X, Ding Y et al (2010) Electrochemical determination of nitrobenzene using bismuth-film modified carbon paste electrode in the presence of cetyltrimethylammonium bromide. Anal Methods 2:1095–1100

Ma J, Zhang Y, Zhang X et al (2012) Sensitive electrochemical detection of nitrobenzene based on macro-/meso-porous carbon materials modified glassy carbon electrode. Talanta 88:696–700

Marcano DC, Kosynkin DV, Berlin JM (2010) Improved synthesis of graphene oxide. ACS Nano 4:806–4814

Neo CY, Ouyang J (2013) Ethyl cellulose and functionalized carbon nanotubes as a co-gelator for high-performance quasi-solid state dye-sensitized solar cells. J Mater Chem A 1:14392–14401

Ouyang W, Sun J, Memon J et al (2013) Scalable preparation of three-dimensional porous structures of reduced graphene oxide/cellulose composites and their application in supercapacitors. Carbon 62:501–509

Palanisamy S, Ramaraj SK, Chen SM et al (2017) A novel Laccase biosensor based on laccase immobilized graphene-cellulose microfiber composite modified screen-printed carbon electrode for sensitive determination of catechol. Sci Rep 7:41214

Qi B, Lin F, Bai J et al (2008) An ordered mesoporous carbon/didodecyldimethylammonium bromide composite and its application in the electro-catalytic reduction of nitrobenzene. Mater Lett 62:3670–3672

Qi H, Schulz B, Vad T, Liu J et al (2015) Novel carbon nanotube/cellulose composite fibers as multifunctional materials. ACS Appl Mater Interfaces 7:22404–22412

Qiu B, Li Q, Shen B et al (2016) Stöber-like method to synthesize ultradispersed Fe_3O_4 nanoparticles on graphene with excellent Photo-Fenton reaction and high-performance lithium storage. Appl Catal B Environ 183:216–223

Rameshkumar P, Viswanathan P, Ramaraj R (2014) Silicate sol–gel stabilized silver nanoparticles for sensor applications toward mercuric ions, hydrogen peroxide and nitrobenzene. Sens Actuat B 202:1070–1077

Rastogi PK, Krishnamoorthi S, Ganesan V (2014) Palladium nanoparticles incorporated polymer-silica nanocomposite based electrochemical sensing platform for nitrobenzene detection. Electrochim Acta 147:442–450

Sadasivuni KK, Kafy A, Kim HC et al (2015) Reduced graphene oxide filled cellulose films for flexible temperature sensor application. Synth Met 206:154–161

Velmurugan M, Karikalan N, Chen SM et al (2017) Studies on the influence of β-cyclodextrin on graphene oxide and its synergistic activity to the electrochemical detection of nitrobenzene. J Colloid Interface Sci 490:365–371

Velusamy V, Palanisamy S, Chen SM et al (2017) Graphene dispersed cellulose microfibers composite for efficient immobilization of hemoglobin and selective biosensor for

detection of hydrogen peroxide. Sens Actuat B. https://doi.org/10.1016/j.snb.2017.05.041

Vimlesh C, Jaesung P, Young C et al (2010) Waterdispersible magnetite-reduced graphene oxide composites for Arsenic removal. ACS Nano 7:3979–3986

Wang GY, Yang LL, Li Y et al (2013) A luminescent 2D coordination polymer for selective sensing of nitrobenzene. Dalton Trans 42:12865–12868

Weng Z, Su Y, Wang DW et al (2011) Graphene–cellulose paper flexible supercapacitors. Adv Energy Mater 1:917–922

Yadav DK, Ganesan V, Sonkar PK et al (2016) Electrochemical investigation of gold nanoparticles incorporated zinc based metal-organic framework for selective recognition of nitrite and nitrobenzene. Electrochim Acta 200:276–282

Zhang Y, Zeng L, Bo X et al (2012a) Electrochemical study of nitrobenzene reduction using novel Pt nanoparticles/macroporous carbon hybrid nanocomposites. Anal Chim Acta 752:45–52

Zhang X, Liu X, Zheng W et al (2012b) Regenerated cellulose/graphene nanocomposite films prepared in DMAC/LiCl solution. Carbohydr Polym 88:26–30

Zhang Y, Bo X, Luhana C et al (2013) A partially reduced C 60-grafted macroporous carbon composite for the enhanced electrocatalysis of nitroaromatic compounds. RSC Adv 3:17300–17306

Zhang Y, Bo X, Nsabimana A et al (2014) Fabrication of 2D ordered mesoporous carbon nitride and its use as electrochemical sensing platform for H_2O_2, nitrobenzene, and NADH detection. Biosens Bioelectron 53:250–256

Zhang C, Zhang RZ, Ma YQ et al (2015) Preparation of cellulose/graphene composite and its applications for triazine pesticides adsorption from water. ACS Sustain Chem Eng 3:396–405

Zhao ZQ, Chen X, Yang Q et al (2012) Selective adsorption toward toxic metal ions results in selective response: electrochemical studies on a polypyrrole/reduced graphene oxide nanocomposite. Chem Commun 48:2180–2182